AUTOMATIC REGISTRATION OF SIMULTANEOUSLY OVERLAPPING IMAGES

James Bolarinwa Olaleye[1], Oluibukun Gbenga Ajayi[2], Olushola Gabriel Omogunloye[3], Joseph Olayemi Odumosu[4], Chika Vincent Okorocha[5]

ABSTRACT

The application of remote sensing has proved to be of tremendous importance over time in earth observation, monitoring and development. Images (the output of a remote sensing process) provide an overview of a particular place and afford the observer the opportunity to extract detailed information that will aid in making informed decisions. However, these images often come in overlapping patches from the sensor and also are of two-dimensional (2D) views. For a holistic perspective and to enable a stereoscopic view of the desired scene of interest, the bit by bit images must be fused together to produce a single image (mosaic). This fusion is the sole thrust of image registration. This study is intended to provide solution to the traditional (manually assisted) image registration by developing a model that performs automatic conjugate point identification, feature match and registration of multiple overlapping images. An approach which makes use of the relationship between the total matched points and final estimated inliers voted for the automatic registration is proposed for the evaluation of the model's accuracy.

Keywords: image registration; mosaicking; transformation functions; conjugate points; pixel; resolution.

1. INTRODUCTION

Image registration is one of the basic image processing operations in remote sensing and digital photogrammetry. By registering the two different images acquired during different times or by different sensors, it can be used in various applications such as motion correction, change detection, image fusion and formation of composite maps [1]. Image registration is the process of spatially matching two images so that corresponding pixels in the two images correspond to the same physical region of the imaged scene. Image registration is an inevitable problem arising in many image-processing applications whenever two or more images of the same scene have to be compared pixel by pixel [2, 3]. In general, registration aims to align two images (the reference image and the observed image) by estimating translation, rotation, and scale. However, because of the inherent relationship between scale and image resolution, current methods tend to separate scale estimation from translation and rotation estimation [4]. To find a match between two images, conventional

1 Professor, Department of Surveying and Geoinformatics, University of Lagos, Nigeria, Ph. +234(0)8024005748, Email: jb_ola@yahoo.com.
2 Assistant Lecturer, Department of Surveying and Geoinformatics, Federal University of Technology, Minna, Ph. +234(0)8036832797, Email: ogbajayi@gmail.com.
3 Senior Lecturer, Department of Surveying and Geoinformatics, University of Lagos, Nigeria, Ph. +234(0)8024005748, Email: gabolushohan@yahoo.com.
4 Assistant Lecturer, Department of Surveying and Geoinformatics, Federal University of Technology, Minna, Ph. +234(0)8022624535, Email: odumossu4life@yahoo.com.
5 Geospatial Manager, Lordsfield - Geoverdict, Lagos, Nigeria, Ph. +234(0)7030486687, Email: chikaokorocha@gmail.com.

Manuscript received on 6th March 2015, reviewed and accepted on 21st September 2015 as per publication policies of *NED University Journal of Research*. Pertinent discussion including authors' closure will be published in September 2016 issue of the Journal if the discussion is received by 28th February 2016.

James Bolarinwa Olaleye is a Professor in the Department of Surveying and Geoinformatics at University of Lagos, Nigeria where he received his Bachelors and Masters in 1981 and 1984, respectively. He received his PhD from University of New Brunswick, Canada in 1992. He is a recipient of Talbart Abrams Medal awarded by American Society for Photogrammetry and Remote Sensing in 1994.

Oluibukun Gbenga Ajayi is an Assistant Lecturer in the Department of Surveying and Geoinformatics at Federal University of Technology, Minna, Nigeria where he received his Bachelors in 2010. He received his Masters in 2014 from University of Lagos, Nigeria. He specialises in digital photogrammetry, remote sensing and GIS.

Olushola Gabriel Omogunloye is a Senior Lecturer in the Department of Surveying and Geoinformatics at University of Lagos, Nigeria. He specialises in geodesy, engineering surveying, adjustment computation, remote sensing and GIS.

Joseph Olayemi Odumosu is an Assistant Lecturer in the Department of Surveying and Geoinformatics at Federal University of Technology, Minna, Nigeria where he received his Bachelors in 2010. He received his Masters from University of Lagos, Nigeria in 2014. He specialises in geodesy, digital photogrammetry and geodynamics.

Chika Vincent Okorocha is Geospatial Manager at Lordsfield – Geoverdict, Nigeria. He received his Bachelors from Federal University of Technology, Minna, Nigeria and Masters from University of Lagos, Nigeria, respectively, in 2010 and 2014.

methods first construct an image pyramid by downscaling the reference image; the observed image is, subsequently, matched at each level by searching the translation and rotation parameters [5, 6]. The level at which the best match is found determines the scale factor between the reference and the observed image. It is to be noted, however, that the scale can only be estimated at fixed levels and independently from other registration parameters. These are the major disadvantages of this approach [7].

Image registration can be broadly categorized into area based (or pixel-based) and feature-based methods [8]. Area-based methods work by directly matching pixel intensities of the two images as a whole. In contrast, feature based methods extract higher-level structures from the two images and finds the corresponding features to perform registration. Therefore, feature-based methods are useful when corresponding features can be reliably detected [8]. However, if the reference image and the observed image are both in low-resolution, accurate detection of corresponding point may be quite challenging.

Most of image registration approaches fall into local or global methods. Local methods are referred to as rubber sheeting or the control-points method. Global methods involve finding a single transformation imposed on the whole image and are also referred to as automatic registration methods. Registration methods can be viewed as different combination of choices for the following four components [9, 10]: (a) feature space; (b) search space; (c) search strategy; and (d) similarity metric.

The feature space extracts the information in the images that is to be used for matching. The search space is the class of transformations which is capable of aligning the images. The search strategy decides how to choose the next transformation from this space, to be tested in the search for the optimal transformation. The similarity metric determines the relative merit for each test. Search continues according to the search strategy until a transformation is found whose similarity measure is satisfactory. The choice and selection of each of these components is a function of the type of variations present in the images [11].

Generally, image registration has two parts: image to object registration and image to image registration. The image to object registration also includes registration of an image onto an existing map for which control points are usually required. Image to image registration seeks to overlay one image on another for comparison or change detection. It could also be to join one image to another as in the production of mosaic. This could also be called edge-matching. For image to image registration, common, pass or conjugate points are needed [7].

2. REGISTRATION PROBLEM

The sequence of image registration is as follows: given two different representations of the same object (or geographical scene), find a transformation function which (when applied to one image) will align (or register) points in that image with corresponding points in the other image of the same scene/object. By using appropriate computational algorithms, a mapping (transformation) function between two images (spatially and with respect to intensity) can be found to produce a new informative image which has functional and structural information. Mathematically, for two-dimensional (2D) datasets (images) of a given size denoted by A_0 and A_1, mapping between these two images can be expressed as Eq. (1).

$$A_1(x, y) = g(A_0(f(x, y))) + e(x, y) \quad (1a)$$

when $e(x, y) = 0$

$$A_1(x, y) = g(A_0(f(x, y))) \quad (1b)$$

where $e(x,y)$ is an error vector (residual) and is said to be zero for a perfect registration, f is a 2D spatial coordinate transformation i.e $(x, y) = f(x, y)$ and g is a one-dimensional (1D) intensity or radiometric transformation. Note that $A_0(x, y)$ and $A_1(x, y)$ each map to their respective intensity values. Registration, therefore, requires finding the optimal f and g, although the spatial transformation is generally the key to the problem [7].

3. METHODOLOGY OF WORK

The step by step procedure of developing the fully automatic registration model is presented in the flowchart shown in **Figure 1**. Some of the components of the methodology are briefly highlighted as follows

1) Feature identification and extraction: The speeded-up robust feature (SURF) algorithm was used for the identification/detection and extraction of the features on both the base and moving images.
2) Feature matching: Builds the relationship between the feature point sets from the reference and floating images. Sum of square difference (SSD) metric was used at a match threshold of 1.0 Scalar vector
3) Model estimation: The model estimation decides the types and parameters that are needed for mapping function. The parameters are computed from the feature pairs from the correspondence built in feature matching
4) Resampling and computation of transformation matrix: The bilinear interpolation was used for the resampling of the pixel-values and computation of non-integer coordinates. RANdom Sampling Consensus (RANSAC) was used to exclude the outliers and to compute the transformation matrix.

The mathematical models of these algorithms have been explicitly formulated and extensively discussed in reference [7]. Meanwhile the considered transformation functions and the image matching strategy have been herein discussed briefly in the forthcoming sections.

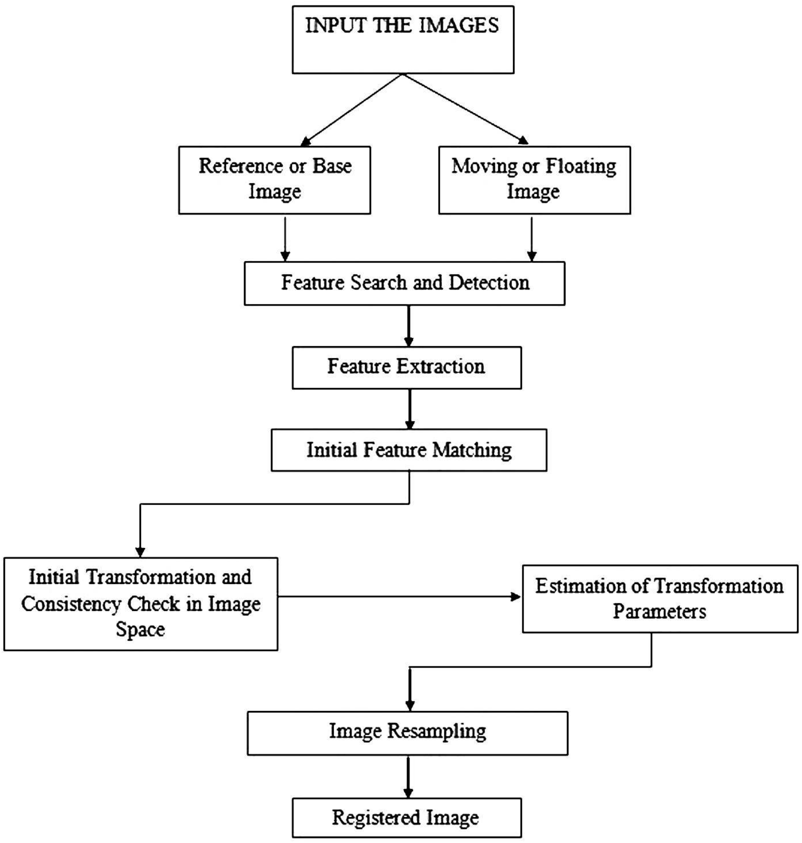

Figure 1. Feature based image registration flowchart.

3.1 Transformation Functions

The type of spatial or geometric transformation needed to properly overlay the input and reference image is one of the most fundamental and difficult tasks in any image registration technique [12]. The establishment of the transformation function that mathematically describes the mapping between imagery in question is a major issue in image registration. In other words, given a pair of images, reference and input images, the transformation function attempts to properly overlay these images. The functions (used to align two images) may be global or local. A global transformation is given by a single set of equations, which optimally registers all the pixels in the two images. Local transformations map the images depending on the spatial location; this results in several sets of equations for one map. Local transformations are usually more accurate but also more computationally demanding [13, 14].

To overcome the problem of geometric distortions, several types of transformation functions have been considered and three of them were used for this study. The 2D conformal transformation (also known as 2D similarity or orthogonal transformation) is sufficient to match two images with rigid-body distortion [9, 10] where the true shape is retained. This is a four-parameter transformation that includes two translations in x- and y-directions, one scale and one rotation. At least two tie points are required to solve for the parameters of the 2D similarity transformation. Mathematically, orthogonal transformation function is given as Eq. (2).

$$x = au + bv + c \tag{2a}$$

$$y = -bu + av + d \tag{2b}$$

Eqs. (2a) and (2b) can be substituted in the matrix notation given by Eq. (3)

$$\begin{bmatrix} x \\ y \end{bmatrix} = \begin{bmatrix} a & b \\ -b & a \end{bmatrix} \begin{bmatrix} u \\ v \end{bmatrix} + \begin{bmatrix} c \\ d \end{bmatrix} \tag{3}$$

where a = cosα; b = sinα; c = T_x; d = T_y; α is the rotation angle; T_x is the translation along x-axis; and T_y is the translation along y-axis.

The affine is a six parameter transformation with the following unknown parameters: *a, b, c, d, e, f*. Each transformation requires a minimum number of reference points (three for affine, six for second order and nine for third order polynomials). If more points are selected, the residuals and the derived root mean square error (RMSE) or sigma may be used to obtain the best estimates.

$$\begin{bmatrix} x \\ y \end{bmatrix} = \begin{bmatrix} a & b \\ c & d \end{bmatrix} \begin{bmatrix} u \\ v \end{bmatrix} + \begin{bmatrix} e \\ f \end{bmatrix} \tag{4}$$

where $\begin{bmatrix} a & b \\ c & d \end{bmatrix}$ are scalar quantities and $\begin{bmatrix} e \\ f \end{bmatrix}$ are the translation parameters.

The affine transformation function modifies the orthogonal type by using different scale factors in x- and y-directions. It applies correction for shrinkage by means of scale factor, applies the translation to the shift of the origin and also performs rotation through angle θ (plus a small angular correction for non-orthogonality to orient the axes in the (u,v) photo system). Unlike orthogonal projection, affine projection allows oblique projection to an image plane [15, 16].

The relational/projective transformation exactly describes a deformation of a flat scene photographed by a pin-hole camera, the optical axis of which is not perpendicular to the scene [8]. It is an eight parameter transformation, which enables the analytical computation of the (u,v) coordinates of the points after they have been projected into a plane from another non-parallel plane and can be expressed by the operator given in Eq. (5).

$$\eta = \phi \begin{bmatrix} a, b, c, d \\ e, f, g, h \end{bmatrix} \tag{5}$$

The transformation can be written as Eq. (6).

$$\begin{bmatrix} x \\ y \end{bmatrix} = \frac{1}{t}\begin{bmatrix} a & b \\ d & e \end{bmatrix}\begin{bmatrix} u \\ v \end{bmatrix} + \frac{1}{t}\begin{bmatrix} c \\ f \end{bmatrix} \tag{6}$$

where $t = gx + hy + 1$; $x = \dfrac{ax + by + 1}{gx + hy + 1}$; and $y = \dfrac{dx + cy + 1}{gx + hy + 1}$

3.2 Image Matching Strategy

Sum of squared difference was used for the correlation and matching of the extracted conjugate points. This algorithm measures the similarity between image templates by taking the sum of pixel differences between each pixel in the reference template (A) and the corresponding pixel in the compared template (B). The summation of these differences creates a simple metric of template or block similarity [Eq. (7)]. It is expected that if the two overlapping images (left and right images) are perfectly matched, the resultant SSD will be equal to zero.

$$SSD\,(i,\ j) = \sum_{m=0}^{M} \sum_{n=0}^{N} (A(i+m,\ j+n) - B(m,\ n))^2 \tag{7}$$

SSD works by shifting the template over the reference image (A) to find the best match. For example, shifting the template to different positions on the reference image until the best matching area or position is found. It should also be noted that a good match is said to be found when the computed SSD is equal to zero. **Figure 2** is a block flow showing the major stages of computing SSD. The working of SSD algorithm can be demonstrated with the help of following example.

3.2.1 Example

Suppose that

$A = \begin{array}{|c|c|c|} \hline 3 & 4 & 2 \\ \hline 7 & 1 & 3 \\ \hline 2 & 3 & 6 \\ \hline \end{array}$ and $B = \begin{array}{|c|c|} \hline 1 & 3 \\ \hline 3 & 6 \\ \hline \end{array}$

In order to find the best match between A and B, four cases have been considered. The region highlighted in red colour is the region under consideration.

Case # 1:

$A_1 = \begin{array}{|c|c|c|} \hline 3 & 4 & 2 \\ \hline 7 & 1 & 3 \\ \hline 2 & 3 & 6 \\ \hline \end{array}$

The difference between the shaded region and the template is

$A_1 - B = \begin{array}{|c|c|} \hline 3 & -1 \\ \hline -2 & -3 \\ \hline \end{array}$

The square of the difference between the shaded region and the template is

$(A_1 - B)^2 = \begin{array}{|c|c|} \hline 9 & 1 \\ \hline 4 & 9 \\ \hline \end{array}$

SSD of the shaded region and the template is

$\Sigma\,(A_1 - B)^2 = 9 + 1 + 9 + 4 = 23$

Compute The Difference between the conjugate points. i.e: $A(i+m, j+n) - B(m,n)$ → Find the Squared Value of the computed Difference. i.e: $(A(i+m, j+n) - B(m,n))^2$ → Compute the Summation of the squared differences i.e: $\sum_{m=0}^{M}\sum_{n=0}^{N}(A(i+m, j+n) - B(m,n))^2$

Figure 2. Computation stages of SSD.

Since 23 $\neq$ 0, this shaded region is not a good match for the template.

Case # 2:

$$A_2 = \begin{array}{|c|c|c|}\hline 3 & 4 & 2 \\ \hline 7 & 1 & 3 \\ \hline 2 & 3 & 6 \\ \hline \end{array}$$

The difference between the shaded region and the template is

$$A_2 - B = \begin{array}{|c|c|}\hline 0 & 0 \\ \hline 0 & 0 \\ \hline \end{array}$$

The square of the difference between the shaded region and the template is

$$(A_2 - B)^2 = \begin{array}{|c|c|}\hline 0 & 0 \\ \hline 0 & 0 \\ \hline \end{array}$$

SSD of the shaded region and the template is

$$\Sigma\ (A_2 - B)^2 = 0 + 0 + 0 + 0 = 0$$

Since 0 = 0, this shaded region can be said to be good match for the template.

Case # 3:

$$A_3 = \begin{array}{|c|c|c|}\hline 3 & 4 & 2 \\ \hline 7 & 1 & 3 \\ \hline 2 & 3 & 6 \\ \hline \end{array}$$

The difference between the shaded region and the template is

$$A_3 - B = \begin{array}{|c|c|}\hline 6 & -2 \\ \hline -1 & -3 \\ \hline \end{array}$$

The square of the difference between the shaded region and the template is

$$(A_3 - B)^2 = \begin{array}{|c|c|}\hline 36 & 4 \\ \hline 1 & 9 \\ \hline \end{array}$$

SSD of the shaded region and the template is

$$\Sigma\ (A_3 - B)^2 = 36 + 4 + 9 + 1 = 50$$

Since 50 $\neq$ 0, this shaded region is not a good match for the template.

Case # 4:

$$A_4 = \begin{array}{|c|c|c|}\hline 3 & 4 & 2 \\ \hline 7 & 1 & 3 \\ \hline 2 & 3 & 6 \\ \hline \end{array}$$

The difference between the shaded region and the template is

$$A_4 - B = \begin{array}{|c|c|}\hline 2 & 1 \\ \hline 4 & -5 \\ \hline \end{array}$$

The square of the difference between the shaded region and the template is

$$(A_3 - B)^2 = \begin{array}{|c|c|}\hline 4 & 1 \\ \hline 16 & 25 \\ \hline \end{array}$$

SSD of the shaded region and the template is

$$\Sigma\ (A_4 - B)^2 = 4+1+25+16 = 46$$

Since 46 $\neq$ 0, this shaded region is not a good match for the template.

3.3 Building Graphic User Interphase

For presentable packaging and to ensure interaction between the model and the user, a simple and user-friendly graphic user interphase (GUI) was constructed and designed to harmonise all the written scripts (programme codes). The GUIDE builder within the MATLAB environment was used for the GUI design.

4. EXPERIMETNAL RESULTS

The results obtained from the developed model for geometric based registration using three transformation models are discussed in the forthcoming sections.

4.1 Graphical User Interphase of Model

Figure 2 shows the screen shot of the GUI developed for the model to aid user interaction with the model and for easy manipulation.

4.2 Model Experimentation

The images used for the model experimentation are images showing aerial view of part of the University of Lagos, Akoka Campus, Nigeria. They were extracted from Google Earth Pro which is a real time online images provider. Some of the images to be registered are presented as **Figures 3a** and **3b**.

Figure 3a. Image of part of UNILAG campus (base image).

Figure 3b. Image of part of UNILAG campus (moving image).

4.2.1 Registration using non-reflective similarity transformation function

Figure 4a shows the automatic conjugate points identification and extraction (with inliers and outliers) while **Figure 4b** presents the automatically extracted conjugate points used for the computation of the transformation matrix (outliers excluded). **Figure 4c** shows the final registered image of the two overlapping images using non-reflective transformation function. The computed transformation matrix (T) is given below. The estimation of accuracy measure comes out to be 20.1111 percent.

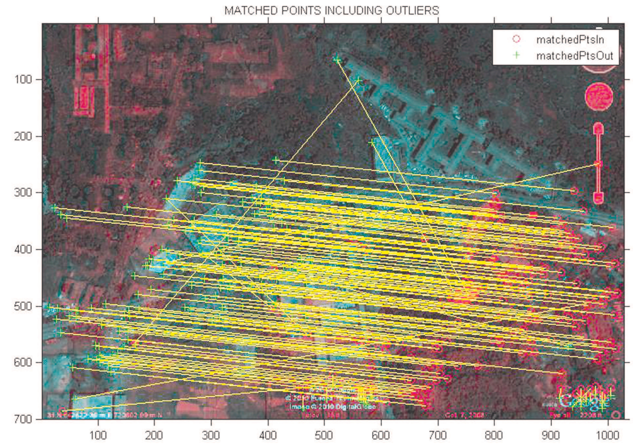

Figure 4a. All matched points (using non reflective similarity transformation function).

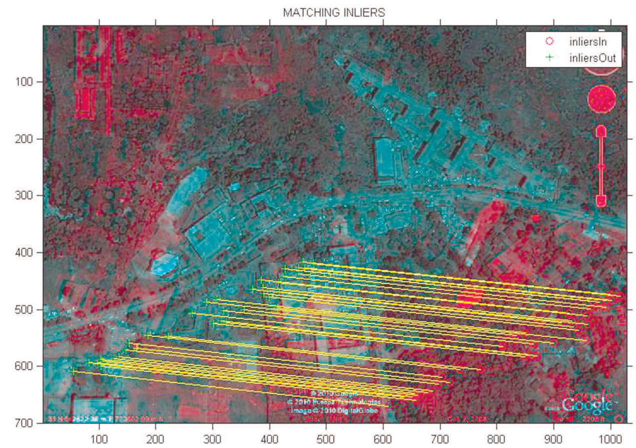

Figure 4b. Image of inliers used for computation of transformation matrix and final registration.

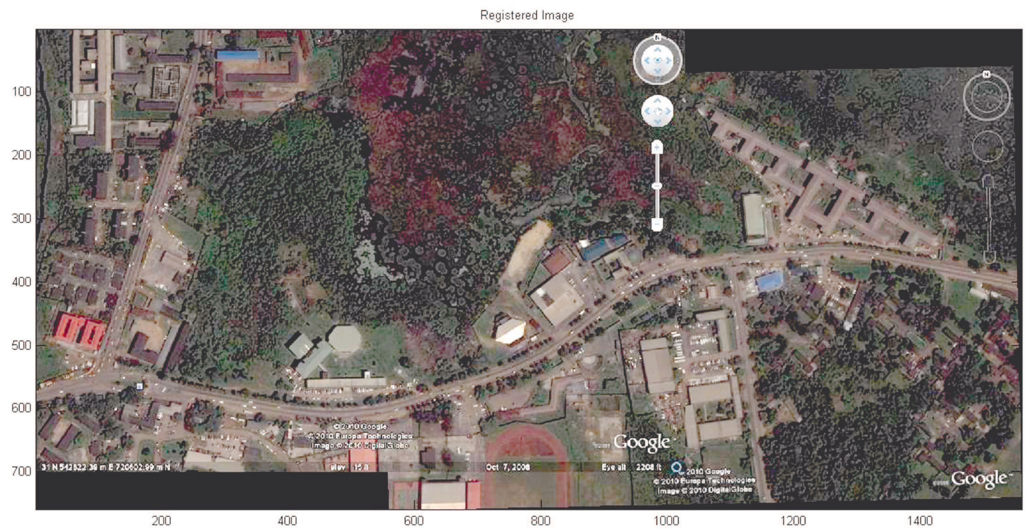

Figure 4c. Registered image of two overlapping images using non-reflective similarity transformation function.

$$T = \begin{bmatrix} 0.9752 & 0.0198 & 543.4348 \\ -0.0198 & 0.9752 & 77.0953 \\ 0.0000 & 0.0000 & 1.0000 \end{bmatrix}$$

4.2.2 Using affine transformation model

The results obtained from the process of using affine transformation function are as shown in **Figures 5a-c**. **Figure 5a** shows the automatic conjugate point identification and extraction (inliers and outliers). **Figure 5b** shows the inliers used for the final computation of the transformation matrix. **Figure 5c** shows the final registered image of the two overlapping images using affine transform. The computed transformation matrix is given below. The estimation of accuracy measure comes out to be 61.9576 percent.

$$T = \begin{bmatrix} 1.0023 & 0.0731 & 508.4306 \\ -0.0005 & 1.0163 & 50.6341 \\ 0.0000 & 0.0000 & 1.0000 \end{bmatrix}$$

4.2.3 Using projective transformation

The results obtained from using the projective transformation function for the automatic registration are as shown in **Figures 6a-c**. **Figure 6a** shows the automatic conjugate point identification and

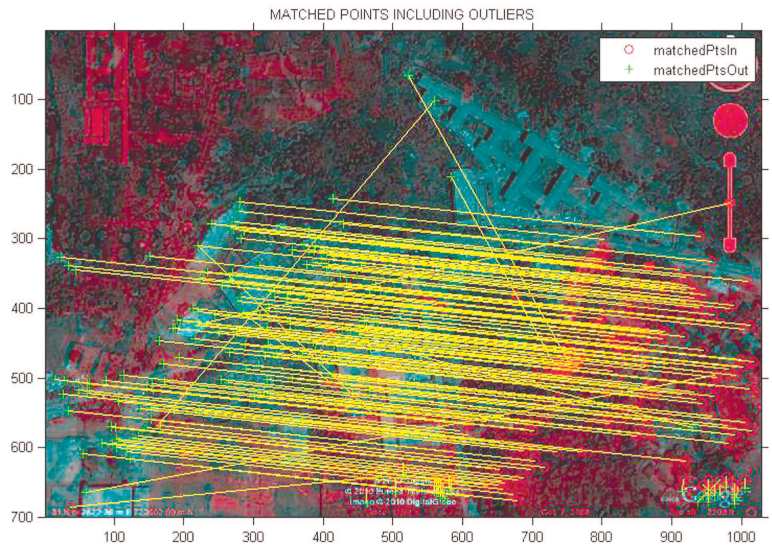

Figure 5a. Image of all matched points including outliers (using affine transformation function).

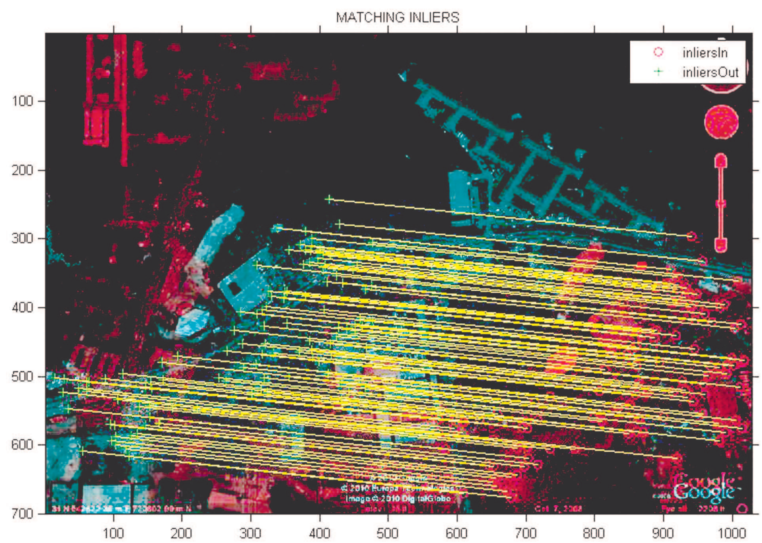

Figure 5b. Image of inliers used for computation of transformation matrix and final registration.

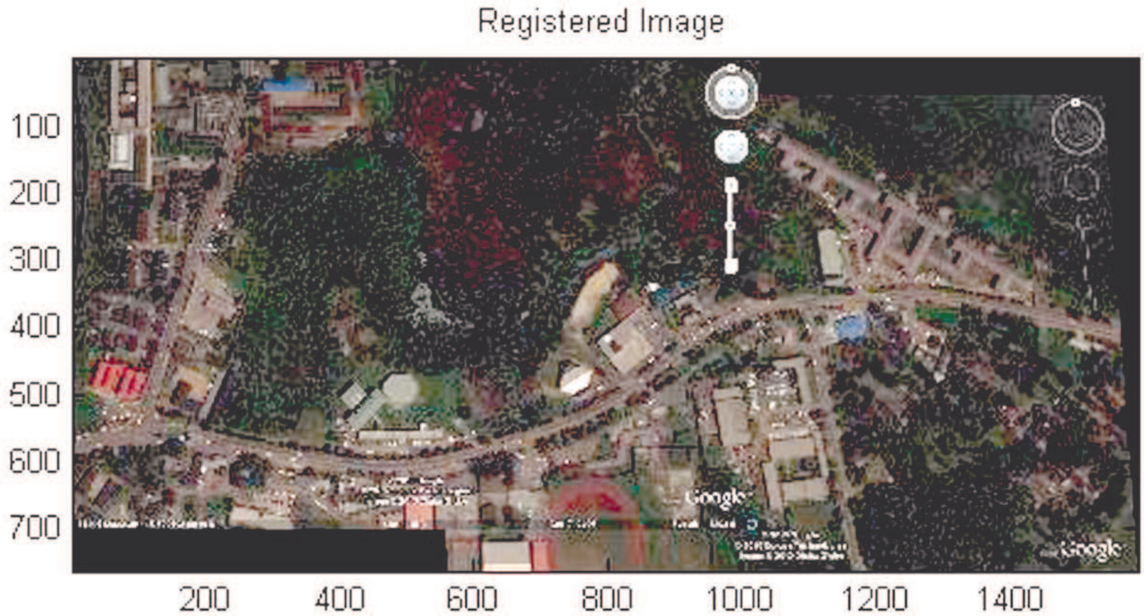

Figure 5c. Registered image of two overlapping images using affine transformation.

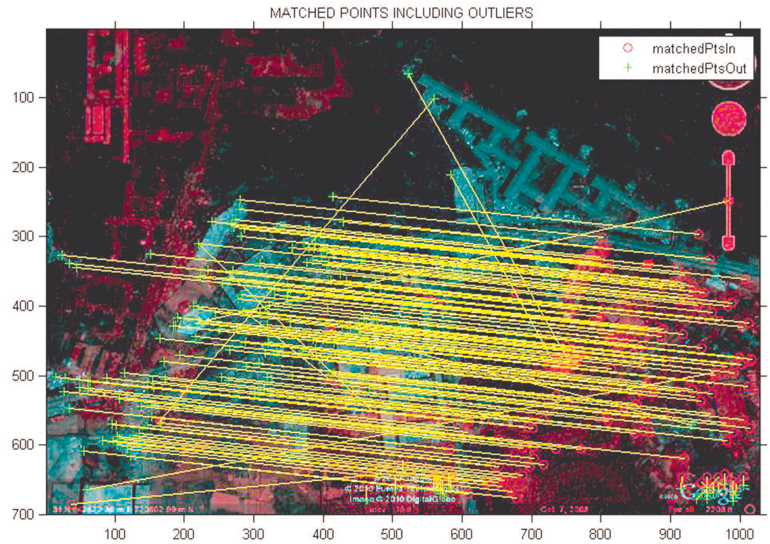

Figure 6a. Image of all matched points including outliers (using projective transformation).

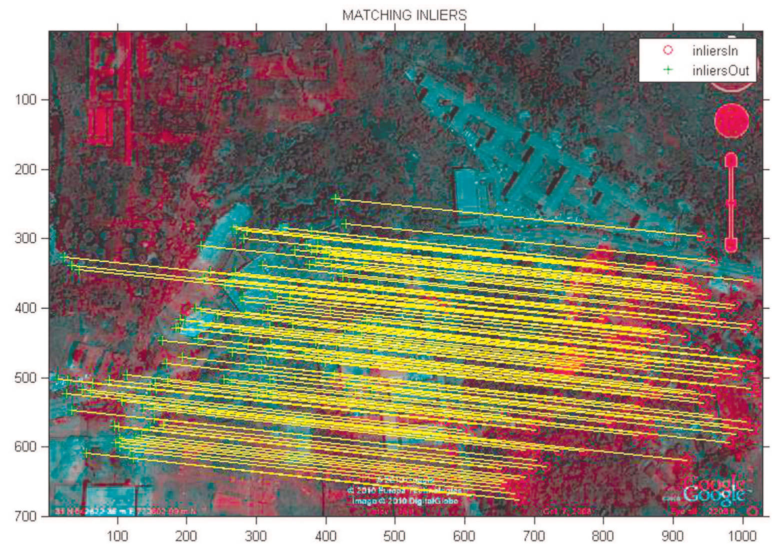

Figure 6b. Image showing only inliers used for computation of transformation matrix and final registration.

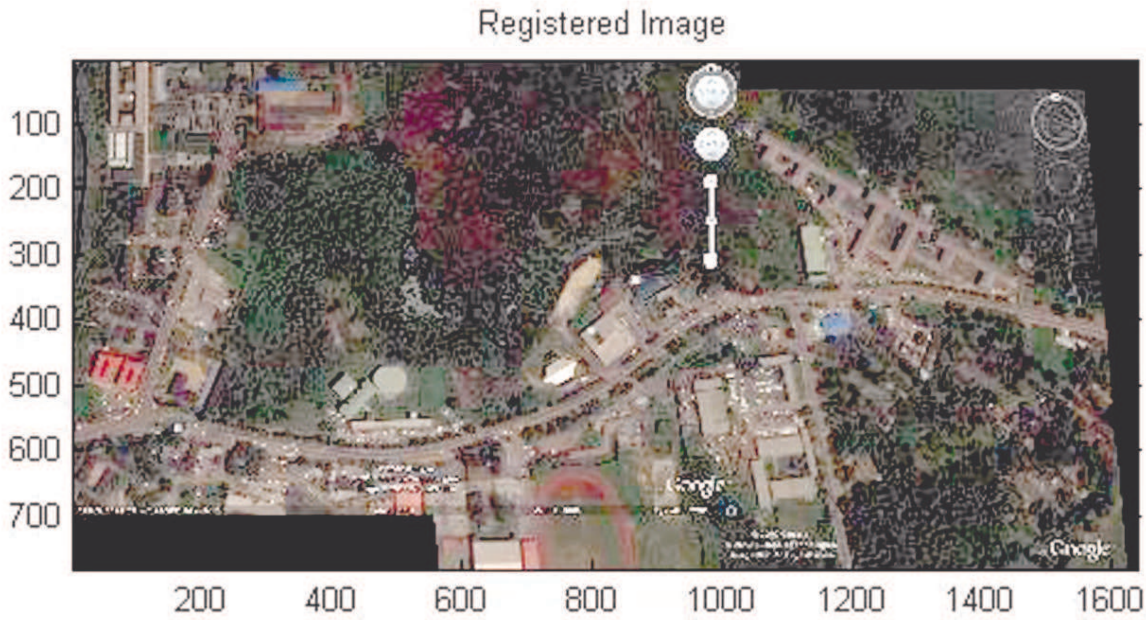

Figure 6c. Registered image of two overlapping images using projective transformation.

extraction (inliers and outliers). **Figure 6b** shows the inliers used for the final computation of the transformation matrix. **Figure 6c** shows the final registered image of the two overlapping images using projective transformation function. The computed transformation matrix is given below. The estimation of accuracy measure comes out to be 75.0007 percent.

$$T = \begin{bmatrix} 1.0333 & 0.1185 & 496.2473 \\ 0.0015 & 1.0588 & 41.9808 \\ 0.0000 & 0.0000 & 1.0000 \end{bmatrix}$$

4.2.4 Automatic registration of three overlapping images using projective transformation

The results obtained from the process of using projective transformation function for the registration of three overlapping images are as shown in **Figures 7a-c**. **Figure 7a** shows the automatic conjugate point identification and extraction (inliers and outliers). **Figure 7b** shows the inliers used for the final computation of the transformation matrix. **Figure 7c** shows the final registered image of the three overlapping images using projective transform. The computed transformation matrix is given below. The accuracy estimation of the three overlapping images using projective transformation comes out to be 72.5011 percent.

$$T = \begin{bmatrix} 0.6982 & 0.0282 & 620.5997 \\ 0.0024 & 1.6998 & 43.0431 \\ 0.0000 & 0.0000 & 1.0000 \end{bmatrix}$$

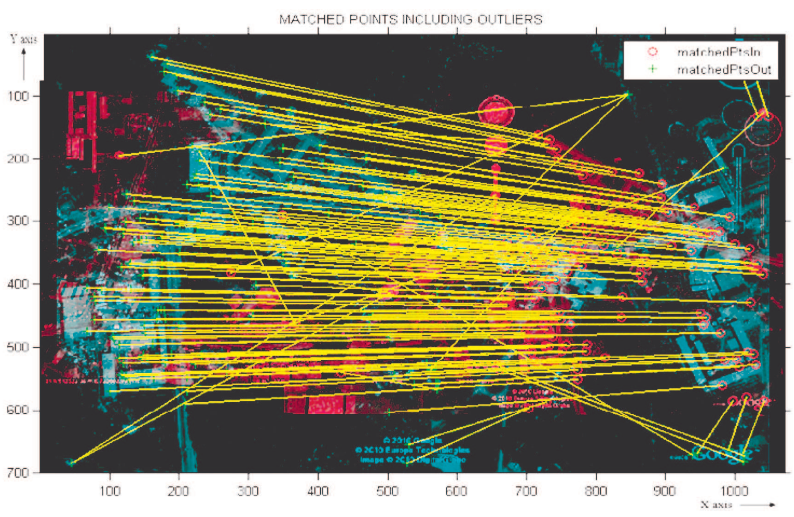

Figure 7a. Image of inliers and outliers of three overlapping images using projective transformation.

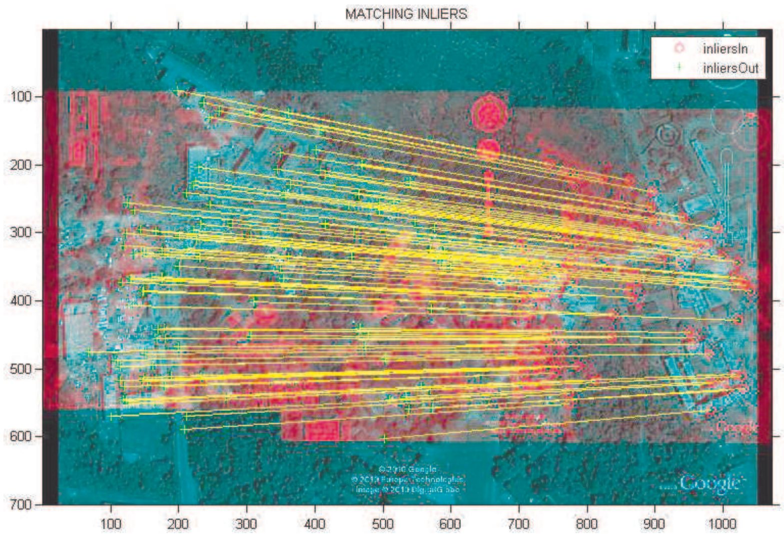

Figure 7b. Image of matched inliers of three overlapping images using projective transformation.

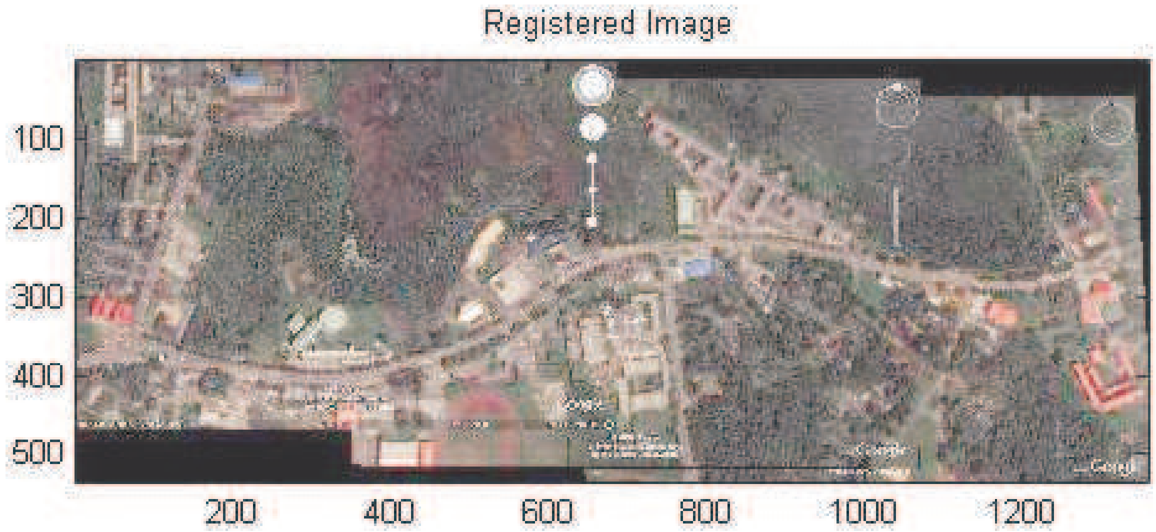

Figure 7c. Three registered overlapping images using projective transformation function.

4.2.5 Automatic registration of four overlapping images using projective transformation

Attempt was made during the experimentation to register four overlapping images by applying projective transformation function using the developed MATLAB model and the results obtained are presented in **Figure 8**. The computed transformation matrix is given below. The estimated accuracy comes out to be 83.7838 percent.

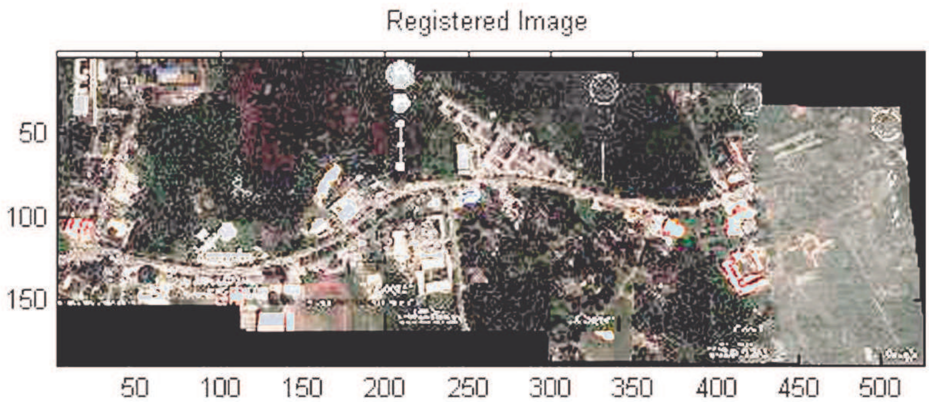

Figure 8. Four overlapping images registered using developed model (based on projective transformation function).

$$T = \begin{bmatrix} 0.2285 & 0.0128 & 280.3468 \\ 0.0035 & 0.2223 & 29.5582 \\ 0.0000 & 0.0000 & 1.0000 \end{bmatrix}$$

5. DISCUSSION ON RESULTS

The corresponding relationship that exists between all the matched points (outliers and inliers) and the matched points obtained after the exclusion of outliers (inliers) only defines the accuracy of the registration process. This indicates the strength and robustness of the statistical tool used for the exclusion of outliers and the computation of transformation matrix. The statistical tool uses the inliers obtained after the exclusion of the outliers to compute the transformation matrix which is the backbone of the registration. RANSAC was used for the exclusion of the outliers (to sieve out the outliers or destructive errors and mismatch) and the computation of transformation matrix. It is a very robust and dependable statistical tool.

Deductions from the results of the feature based automatic registration obtained shows that projective transformation model gave the highest estimation of accuracy with approximate accuracy ranging from 75-84 percent. This is followed by the affine based transformation registration with an accuracy of approximately 62 percent. The lowest accuracy was obtained from the registration process which used non-reflective similarity transformation model with an accuracy estimation of approximately 20 percent. The accuracy obtained is basically a function of the statistical tools used for SURF, feature match (SSD metric), similarity measure, interpolation and resampling (bilinear interpolation), exclusion of outliers and computation of transformation matrix (RANSAC), the radiometric and geometric resolution of the image amongst other factors. The degree of overlap in both images is also very important.

5. CONCLUSIONS

1) Efficiency and accuracy is a function of the degrees of freedom of the transformation matrix. The more numbers of degree of freedom as presented by the transformation technique, the more flexible registration becomes which improves the registration efficiency and the resultant accuracy. The result obtained from the registration process in which projective transformation was used (with eight degrees of freedom) produced an accuracy which is better than the accuracy obtained from affine based transformation model. The result obtained from the affine-based registration algorithm also proved to be more accurate than those obtained from the registration process which used non-reflective similarity transformation model.
2) SURF was adopted for the feature detection and feature extraction. Feature matching was done using the SSD metric with the matchthreshold set at 1.0 scalar value, the feature vectors were normalized to unit vectors before computation. Bilinear interpolation was used for resampling and computation of non-integer coordinates which is commonly implemented by convolving the input image separately in the x- and y- directions with a triangle weighting function while RANSAC was used for the exclusion of the outliers and the computation of the transformation matrix.
3) The time taken by the registration process and the accuracy obtained are both directly proportional to the radiometric and geometric properties (e.g. resolution) of the image. The automatic registration model took 42-62 sec during the experimentation.
4) The speed of the developed model is also a function of the nature and size of the images to be registered and also the configuration of the operating system computer used.

Further research focus will concentrate on investigating the robustness of epipolar geometry in automatic registration of overlapping images. The robustness of other feature detection, extraction and image matching models will also be examined.

REFERENCES

[1] Kumar AS, Manjunath AS, Rao KMM. Merging IRS Multispectral and PAN images by A-Trous Wavelets. Int J Remote Sens 2003;24(12): 2387-2582.

[2] Xiaolong D, Siamak K. A Feature-Based Image Registration Algorithm Using Improved Chain-Code Representation Combined with Invariant Moments. IEEE Trans Geosci Remote Sens 1999;37(5):2351-2362.

[3] Zhang P-f, Li X-y, Ma L. Grid Computing based on Game Optimization Theory for Networks Scheduling. J Network 2014;9(5):1295-1300.

[4] Dufournaud Y, Schmid C, Horaud R. Matching Images With Different Resolutions. In: Proceedings of IEEE Conference on Computer Vision and Pattern Recognition. South Carolina, USA: 2000. p. 612-618.

[5] Bovick AC. Essential guide to image processing. Academic Press, Elsevier Inc, 2009. 381 p.
[6] Adelson EH, Anderson CH, Bergen JR, Burt PJ, Ogden JM. Pyramid Methods in Image Processing. RCA Eng 1984;29(6):33-41.
[7] Ajayi OG. An Iterative MATLAB Program for the Automatic Registration of Overlapping Images. MSc thesis. University of Lagos, Nigeria, 2014.
[8] Barbara Z, Flusser J, Image Registration Methods: A Survey, Image and Vision Computing 2003;21(11):977-1000.
[9] Brown LG. A Survey of Image Registration Techniques. Comp Surv 1992;24(4):325-376.
[10] Dung L, Huang C, Wu Y. Implementation of RANSAC Algorithm for Feature-Based Image Registration. J Comp Commun 2013;1(1):46-50.
[11] Rao CR, Rao KMM, Manjunath AS, Srinivas RVN. Optimization of Automatic Registration Algorithm and Charaterization. PS Comission III, WG, III/8, 2012.
[12] Al-Ruzouq R. Semi-Automatic Registration of Multi-Source Satellite Imagery with Varying Geometric Resolutions. PhD thesis. University of Calgary, Canada, 2004.
[13] Fonseca LMG, Manjunath BS. Registration Techniques for Multi Sensor Remotely Sensed Imagery. Photogramm Engg Remote Sens 1996;562(9):1049-1056.
[14] Xia Y, Tang X. Extracting Method of Control Point Pairs for Remote Sensing Image Based on Regional Matching. Int J Sig Process, Image Process Pattern Recog 2013;6(2):145-154.
[15] Stamatopoulos C, Fraser CS. An Orthogonal Projection Model for Photogrammetric Orientation of Long Focal Length Imagery. In: AfricaGEO. Cape Town, South Africa: 2011.
[16] Ajayi OG, Odumosu JO, Okorocha CV, Nzelibe IC, Ahmadu HA, Bawa S. Semi-Automatic Generation of Mosaic From Overlapping Images Using MATLAB. Int J Engg Advance Tech Studies 2014;2(4):1-15.